Assessment of the grid requirements for the modelling of the dynamics of high speed evaporating sprays using LES / Eulerian-Lagrangian frameworks

C. Li, C. Crua, R. Morgan and K. Vogiatzaki*
Advanced Engineering Centre, University of Brighton, UK

Abstract

The physics of high speed liquid jets injected in elevated temperature and pressure conditions are extremely complex due to the multi-scale and multi-phase flow characteristics. Large eddy simulations (LES) are widely applied for simulations of multi-phase flows because large scale mixing of ambient air with the liquid vapour (when evaporation is occurring) is better captured than other traditional CFD techniques, such as Reynolds Averaged Navier-Stokes. However, in order the LES predictions to be accurate, in addition to the required numerical accuracy of the solvers and the effect of sub-grid scale (SGS) models, the mesh dependence needs to be addressed when the mesh refinement is not enough due to limited computing resources. This work uses as the basis for our analysis fuel spray simulations of n-dodecane under non-reacting conditions injected in a high pressure, high temperature constant chamber known as "Spray A". Although previous works have presented the effect the grid has on the accuracy of the results based on "trial and error" basis, no insight of the dynamics of each phase was provided in the same conditions under different grids. In our work the novelty lies in the fact that the observed trends of each phase regarding to the mesh size are explained based on the code numerics and linked to the physics of the flow. It aimes to improve the understanding of the role of mesh refinement in multi-phase coupling characteristics and to provide a guideline for mesh resolution requirements of high speed evaporating sprays within LES/Eulerian Lagrangian approaches.

Introduction

In energy systems operating with high pressure liquid fuel injection, such as internal combustion (IC) engines, the fuel air mixing is strongly affected by the turbulent nature of the flow inside the combustion chamber. Direct Numerical Simulations (DNS) offer the potential to fully resolve all the relevant flow scales, however, the computational cost involved is not practical for industrial scale systems. Reynolds Averaged Navier Stokes (RANS), is a commonly employed method for industrial simulations. It models all scales of turbulence and the results can be seen as a time averaged description of the flow field. The mesh resolution is not an unknown factor for optimising the simulations since grid independence can and should occur after a certain level of refinement. A number of studies have been conducted recently using RANS for validation of modelling capability of Spray A conditions [1, 2] and fuel mixing under complex injection conditions[3]. Simulating directly the large scales of turbulence rather than modelling them gives a higher degree of detail and allows a more advanced analysis of the physical problem. Large eddy simulations (LES) are widely applied for complex multi-phase flows and can obtain levels of predictability that can not be achieved by the traditional RANS technique. In addition to the higher required numerical complexity of LES solvers and the sub-grid scale models (SGS), the mesh dependence issue needs also to be addressed. The major challenge is that the grid convergence concept in LES, especially for multi-phase flows is hard to be defined with strict criteria similar to single phase flows based on the Kolmogorov and Taylor scales analysis since the presence of multiple phases imposes a wider range of scales. Many studies have examined the effect of grid resolution for simulations of Spray A conditions using various commercial softwares (for example, KIVA [4], CONVERGE [5, 6] and OpenFOAM [7, 8]) in combination with various spray models. The common practice of increasing the mesh resolution or tuning the spray coefficients in order to capture the small scale structures and to improve the convergence of results against the experimental data is implemented. This approach, although gives accurate simulation results, however is not predictive and a criterion needs to be established as to what should be the grid requirements. For the case of Spray A various grids have been examined and a minimum grid size of $0.125mm$ has been reported to capture the flow coherent structures [5, 6]. However, none of these studies has provided a physical and numerical explanation as to why this is the desirable resolution or an explanation of the observed trends in the results because of the gird refinement. In the present study, a detailed analysis of the dependence of mesh resolution and its principles for simulating multiphase flow using LES in practical engineer applications is presented. Spray simulations are carried out using LES and Eulerian/Lagrangian Particle Tracking

*Corresponding author: K.Vogiatzaki@brighton.ac.uk

(LPT) methods [9]. The background motivation for the study is to explore the limitations, possibilities and challenges that come with grid changes within the LPT method in high resolution LES and to establish a criterion as to how we should define the grid requirements within Eulerian-Lagrangian frameworks.

Spray and LES Models

The simulations were performed using the Eulerian-Lagrangian approach in OpenFOAM. The ReitzKHRT model which is a combination of Kelvin-Helmholtz (KH) and Rayleigh-Taylor (RT) models is used to predict the subsequent secondary droplet breakup [10, 11]. The Spalding evaporation model[12] based on the mass evaporation rate of a single, isolated droplet, evaporating in an infinite, constant temperature and constant velocity air environment is also adopted. Within LES the large, energy-containing eddy structures (filtered quantities) are expected to be resolved on the computational grid, whereas the smaller, more isotropic, sub-grid structures (SGS) are modelled. The effect of the small scales is obtained through the sub-grid scale stress term ($\tau_{ij} = \overline{u_i u_j} - \overline{u}_i \overline{u}_j$) that must be modelled. Previous LES research on the same Spray A condition used the Smagorinsky Model [5, 6], with a constant model coefficient. To avoid using a constant coefficient which should be evaluated a priori, a dynamic one-equation eddy viscosity model is used in present study. Its dynamic procedure can adjust the model coefficient locally and a more accurate effect of the small scales can be applied on the LES flow field.

$T_{ij} = \widetilde{\overline{u_i} \overline{u}_j} - \widetilde{\overline{u}}_i \widetilde{\overline{u}}_j$.

Experimental and Numerical Set Up

Numerical simulations are compared with experiments carried out in a Constant Volume Pre-burn (CVP) vessel chamber facility at Sandia National Laboratories. The specific "Spray A" conditions are provided in table 1. A single component diesel surrogate fuel (i.e., n-dodecane) is used due to its extensively well-characterised chemical and physical properties. The Reynolds (Re) number of the liquid fuel based on the diameter of nozzle and the speed at nozzle is $Re_D = 31,000$.

Ambient gas temperature	900 K
Ambient gas pressure	near 6.0 MPa
Ambient gas density	22.8 kg/m^3
Ambient gas oxygen	0% O2 (non-reacting)
Ambient gas velocity	Near-quiescent, less than 1 m/s
Fuel injector outlet diameter	0.090 mm
Number of holes	1 (single hole)
Discharge coefficient	Cd = 0.86
Fuel	n-dodecane
Fuel injection pressure	150 Mpa
Fuel temperature	363 K (90^{o}C)
Duration of injection (ms)	1.5 ms
Total mass injected (mg)	3.5 mg
Fuel density	750 kg/m^3

Table 1. Summary of Spray A conditions [13].

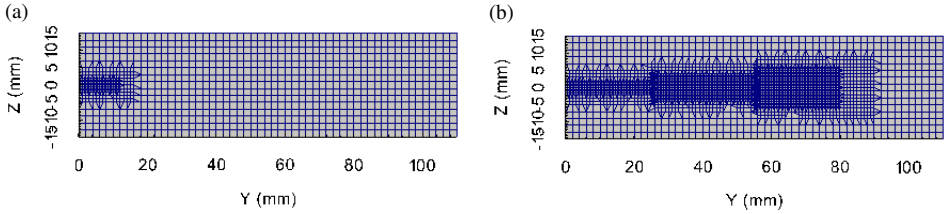

Figure 1. Grid mesh 1 (a) and mesh 2 (b) used for LES simulations of Spray A conditions.

In order to resolve numerically the flow near the injector and along the spray development region, a fixed

grid embedded refinement is employed at two mesh configurations as shown in Figure 1. The first grid (mesh 1) only imposes refinement at the region of the maximum liquid penetration, which based on experimental data is $10mm$. The second grid (mesh 2) is refined in both the liquid and the vapour scales (up to $80mm$). It should be noted that due to the Eulerian-Lagrangian nature of the code the grid affects directly the gas phase and indirectly (through the numerical coupling) the Lagrangian phase. The choice of two different mesh structures allows us to separate the effect of the grid on the liquid/gas coupling from its effect on the vapour development. Three levels of mesh refinement are implemented in the computational domain $-0.015m \leq X \leq 0.015m$, $0 \leq Y \leq 0.11m$, $-0.015m \leq Z \leq 0.015m$.The time step is calculated based on the Courant number criterion: $\mathrm{Co}_{\max} = u\Delta t/\Delta x$ where Δx is the grid size while Δt is the time step. For the calculations presented in the results section the $\mathrm{Co}_{\max} = 0.1$.

Numerical Algorithms

The basis of the two-phase flow code used in this study is the Eulerian-Lagrangian approach in OpenFOAM [14] with necessary modifications to adjust the framework in the LES context. A second-order-accurate spatial discretisation scheme is used for the governing conservation equations. In order to maintain stability, time accuracy is set to first order by running fully implicit. The transport equations are solved using the pressure implicit with splitting of operators (PISO) method. The calculations in this study are run in parallel on distributed memory machines using the message passing interface (MPI). The method of Lagrangian Particle Tracking (LPT) is used to record the movement of liquid parcels as follows: a) Initially each parcel moves until it reaches a cell boundary or for the entire time step dt if it remains in the same cell b) If the parcel changes cell, the time it took to move out of the first cell is calculated and the parcel properties are updated based on this time c) The momentum change is added to the cell that the parcel has been in d) If the parcel still has time left to move, step (a) is repeated. It can be seen that based on this algorithm the grid size apart from its profound role in resolving turbulent scales, it also affects the way the parcels move and how often the momentum equation is updated. It is expected that for smaller grid sizes the parcel properties are updated in shorter time scales than in larger grids although this is also depndent on the simulation time step.

Results and Discussion

Liquid and Vapour penetrations

This section presents the results of spray simulations under Spray A conditions using the two meshes in Figure 1 with different grid resolutions. The spray global characteristics, including liquid and vapour penetrations, are initially compared with experimental data and then a more detailed analysis and explanation of the trends seen at macroscopic level is provided through the analysis of the droplet statistics.

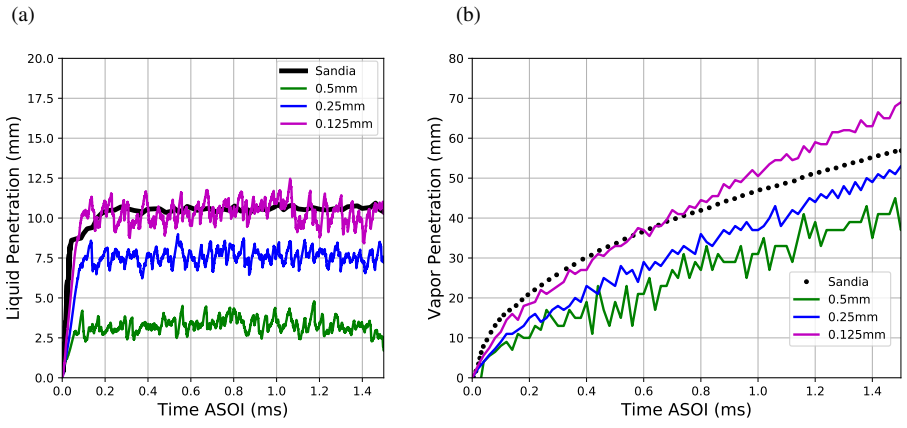

Figure 2. Effect of mesh size on liquid (a) and vapour (b) penetrations for Spray A conditions [13]on mesh 1.

Figures 2 and 3 show the liquid and vapour penetrations as a function of time. The predictions include results from the three different resolutions of mesh 1 (Figure 2) and the two different resolutions of mesh 2 (Figure 3). Note that the grid size in the figures refers to the minimum cell size obtained by mesh refinement. This refinement is only applied to the liquid region (up to 10mm) for mesh 1 and both the liquid and vapour region (up to $80mm$) for mesh 2. The plots show that on the two mesh configurations, $0.5mm$ and $0.25mm$ grid resolutions are not sufficient to reproduce the liquid and vapour penetration characteristics. Liquid is under predicted while vapour

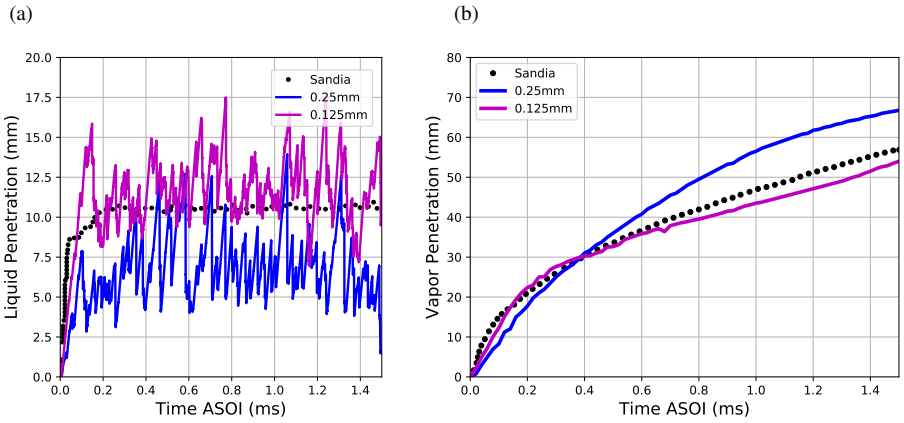

Figure 3. Effect of mesh size on liquid (a) and vapour (b) penetrations for Spray A conditions on mesh 2.

is over-predicted for mesh 1 and under-predicted for mesh 2. For the grid resolution of $0.125mm$, the simulated liquid penetrations approach the experimental data for both mesh configurations. The vapour penetration is also overall well predicted although some important differences are noted between the two different mesh structures for injection time greater than $0.8ms$. Mesh 2 provides higher accuracy which is justified by the fact that in mesh 1 the $0.125mm$ refinement region extends only around the liquid while for mesh 2 the refinement region covers up to $80mm$. These conclusions are consistent with previous studies using different codes [4, 5, 6]. The following sections are focused on further investigations of these observation by examining the effect of mesh resolution on the two phases of Spray A conditions.

Analysis of liquid phase

Figure 4 and 5 show the influence of the mesh size on the development of droplets along the direction of the mass flow injection at two time instances: $t = 0.8ms$ (mid injection duration) and $t = 1.5ms$ (end of injection). A first observation is that the parcels for all grid sizes and mesh structures are experiencing a longer trajectory at $t = 0.8ms$ than $t = 1.5ms$. This is expected since at the end of injection, the injection mass flow rate is reduced to zero, which also results in a lower parcel velocity. Moreover, for all cases, as the grid size is refined the droplet trajectories are longer along the direction of fuel mass injection and more fuel droplets with higher velocities are present. Comparing the end of injection, it can be seen that for grid size $0.25mm$ the liquid penetrates considerably further for mesh 1 rather than mesh 2. However, for grid size 0.125 the liquid penetration is similar for both meshes implying a convergence of the liquid penetration for sufficiently small grid size at the liquid core area.

One way of explaining the previously described behaviour is by using the principle of momentum conservation. Ignoring the exchange of mass at two adjacent short instants, the momentum conservation for gas and liquid phase can be applied in each Eulerian cell:

$$m_p u_{p_A} + \rho_g (dx)^3 u_{g_A} = m_p u_{p_B} + \rho_g (dx)^3 u_{g_B} \tag{1}$$

where m_p, u_{p_A} are the mass and velocity of the particle, ρ_g, dx and u_{g_B} are the density, mesh size and velocity of the gas phase in each cell. When the same amount of momentum $m_p(u_{p_A} - u_{p_B})$ is lost from an active particle in a cell, the acceleration of the passive gas phase within a larger cell size $\rho_g(dx)^3$ is less, and the displacement of gas phase caused by the transferred momentum from liquid particles is shorter. This in turn affects the follow up movement of the parcels and in particular the ones with smaller Stokes numbers. Thus the mesh size has important effect on the moving dynamics of droplets along the direction of mass flow injection, due to momentum conservation between the two phases.

Figure 6 shows the number of parcels against droplet sizes at $t = 1.5ms$ for the two mesh configurations with $0.25mm$ and $0.125mm$. It can be seen that more droplets are observed in the Lagrangian system when the grid size decreases implying potentially more mass, linear momentum as well as linear kinetic energy of moving particles along the direction of mass flow injection with finer mesh. Another interesting observation is that for mesh 2 with both grid resolutions the size of the droplets is on average smaller (around $1.5\mu m$) than mesh 1. Also on mesh 1 the distribution of the droplet sizes is higher than for mesh 2.

The quantity that links the size of the droplets with their dynamic characteristics is the Stokes number. It

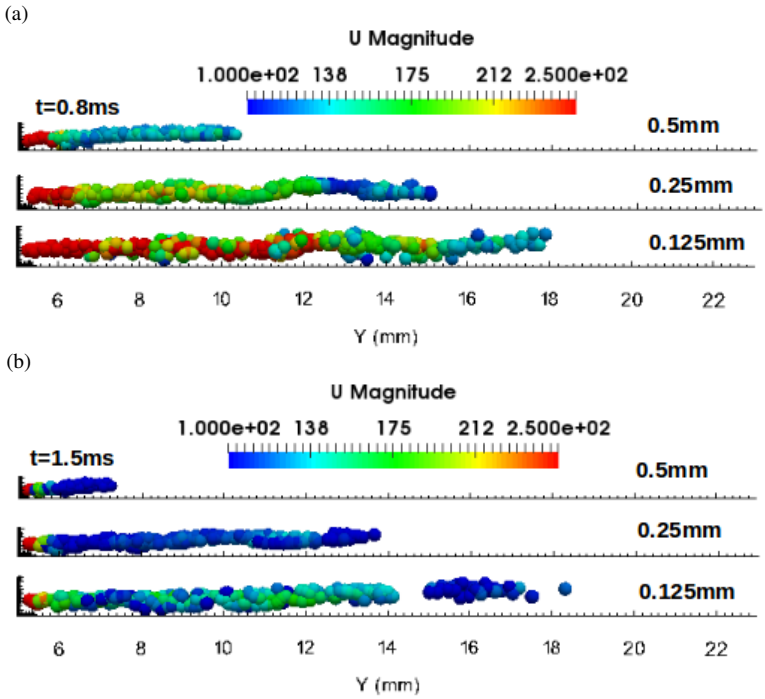

Figure 4. Effect of mesh size on development of particles at $t = 0.8ms$ (a) and $t = 1.5ms$ (b) for Spray A conditions on mesh 1. The parcels are coloured based on the velocity magnitude.

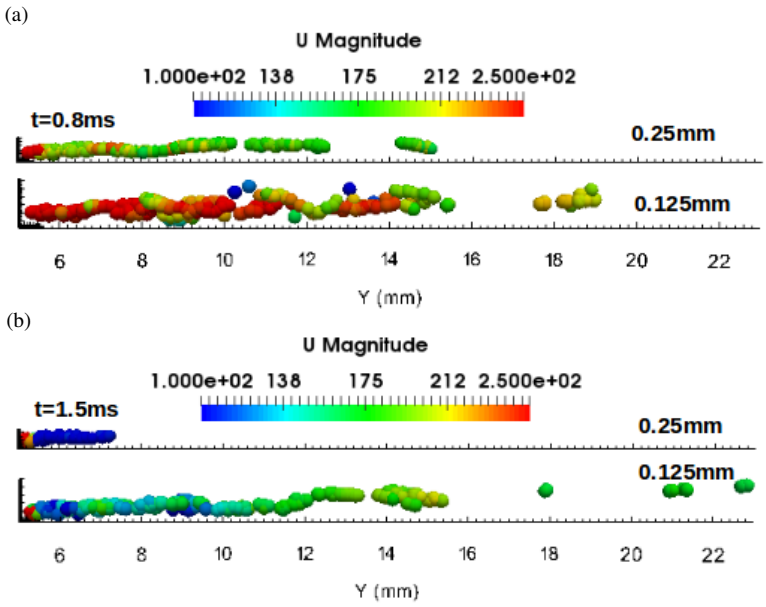

Figure 5. Effect of mesh size on development of particles at $t = 0.8ms$ (a) and $t = 1.5ms$ (b) for Spray A conditions on mesh 2. The parcels are coloured based on their velocity magnitude.

defines the degree to which particle motion is tied to fluid motion. The Stokes number ($S_t = (\rho_p d_p^2 u_s)/(18\mu l_s)$, ρ_p, d_p are density and diameter of droplets, u_s, l_s are the characteristic velocity and length scale of the flow) based on the minimum grid size and the diameter of particles which have the maximum probability in each simulation case in Figure 6 is given in Table 2. It can be seen that the droplets in the simulations using mesh 2 have smaller Stokes number. This means that the droplets in mesh 2 follow fluid streamlines (including motion imposed by turbulence as will be seen in Figure 8) while droplets in mesh 1 are more dominated by their inertia and continue along their initial trajectory. This would explain why in Figure 2 and 3 the particle trajectory is overall longer in mesh 1 than mesh 2 since the particles maintain longer the initial axial momentum they have because of the

injection. Also we can see that for both meshes, as the grid is refined the Stokes number is increased which also explains why the particles penetrate more in finnier grids.

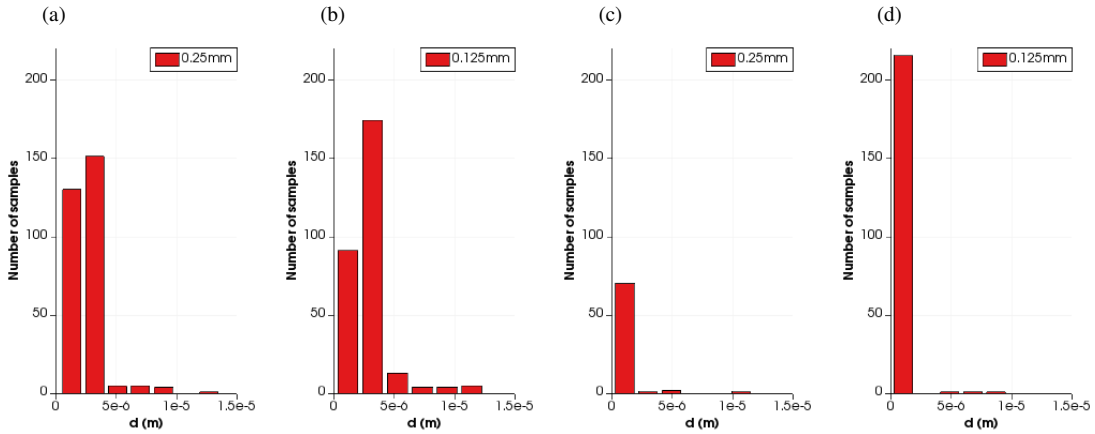

Figure 6. Number of droplets vs droplet sizes at $t = 1.5ms$ for two mesh configurations. (a) $0.25mm$ grid of mesh 1; (b) $0.125mm$ grid of mesh 1; (c) $0.25mm$ grid of mesh 2; (d) $0.125mm$ grid of mesh 2.

case	Stokes number (Sk_o)	Grid size ($dx,\ mm$)	Particle diameter ($d_p, \times 10^{-6}\ m$)
1 (mesh 1)	0.39	0.5	3.2
2 (mesh 1)	0.79	0.25	3.2
3 (mesh 1)	1.58	0.125	3.2
4 (mesh 2)	0.08	0.25	1.0
5 (mesh 2)	0.15	0.125	1.0

Table 2. Summary of Stokes numbers regarding to experimental conditions.

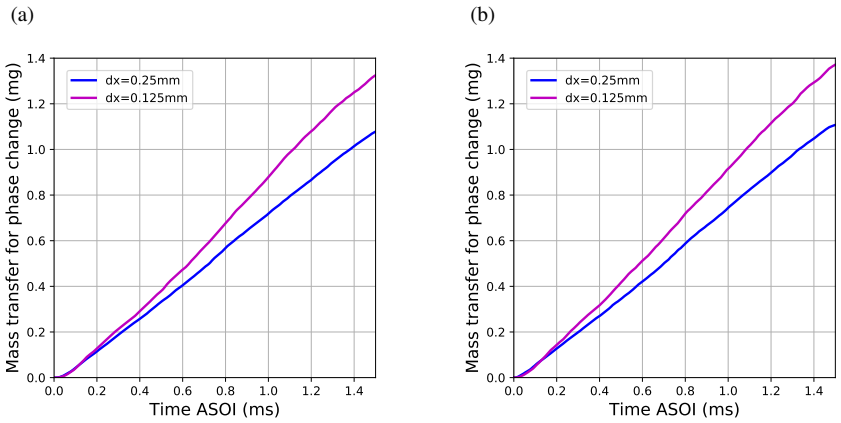

Figure 7. Effect of mesh size on mass transfer for phase change of Spray A conditions for mesh 1 (a) and mesh 2 (b).

Figure 7 shows the total mass transferred due to phase change against time. It can be seen that the amount of fuel mass that undergoes phase change increases as the grid becomes smaller. This is consistent with the observations of Figures.4, 5 since for smaller grid sizes more particles travel "longer" (because they maintain their initial momentum) and continue to evaporate until the injection stops. Moreover, the mass transferred is almost the same amount with the two mesh configurations when the same grid resolution is used, although mesh 2 is more refined downstream along the direction of mass flow injection than mesh 1. This can be an indication that the

total amount of the mass that will change phase depends mostly on the grid refinement close to the nozzle and not further downstream.

Analysis of gas phase

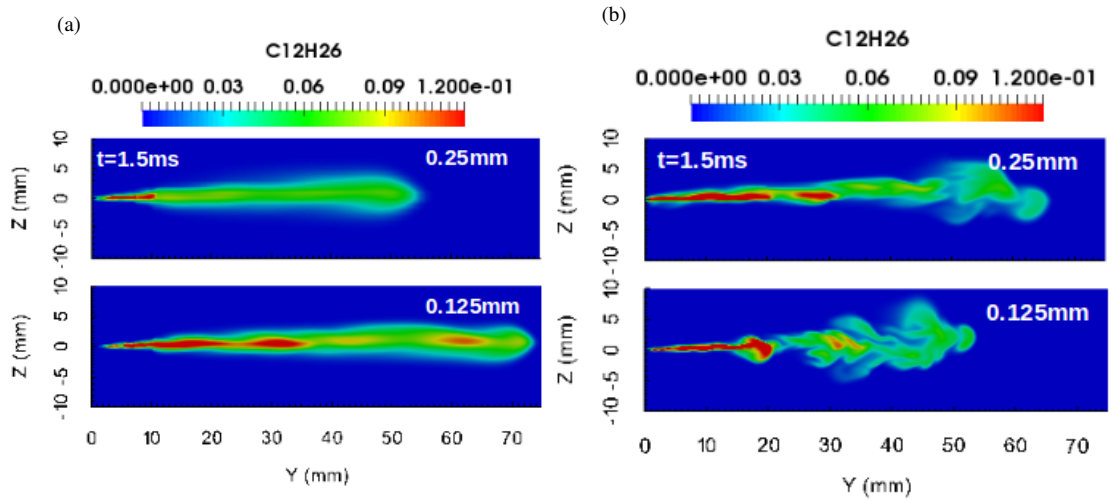

Figure 8. Effect of mesh size on vapour contours at mid-plane $t = 1.5ms$ for Spray A conditions on mesh 1 (a) and mesh 2 (b).

Figure 8 shows the fuel vapour contours at mid-plane at $1.5ms$ for mesh 1 and 2 at two different grid resolutions. It is interesting to notice that although the droplets travel longer as the grid is refined, the same trend is noticed for vapour only for mesh 1 while for mesh 2 the grid refinement causes the vapour to diffuse rather than to penetrate. In the interpretation of the results it should be taken into account that although mesh 1 and mesh 2 have exactly the same resolution in the liquid core part (up to $10mm$) the resolution further downstream is different (see Figure 1). At grid resolution $0.25mm$ the vapour penetration is longer at mesh 2. At grid resolution $0.125mm$ on the other hand the vapour penetration is longer at mesh 1. This behaviour is linked to the effect of small turbulent scales in the process. It appears that although a resolution of $0.125mm$ at the liquid core side (up to $10mm$) is adequate to predict global liquid and vapour penetration and total phase change mass, the instantaneous droplet and vapour characteristics are greatly affected by the resolution further downstream as well, in particular the effect of turbulent eddies at the balance of vapour convection and diffusion. It is estimated that the approximately linear growth trend with decreasing the grid size occurring on liquid penetrations using mesh 1 is mainly a numerical trend dictated by the conservation of momentum (Eq. 1) along the direction of mass flow injection as explained above. On the other hand, the shorter vapour penetration with the $0.125mm$ grid than with $0.25mm$ grid for mesh 2, underlines the physical role of the small scales. In mesh 2 more turbulent scales are included further downstream which increase the mixing of the vapour phase with the surrounding N_2.

It is reminded also that based on Table 2 the numerical Stokes number for mesh 2 are smaller than mesh 1 implying that the droplet trajectories are more prone to change because of the local turbulence. There is a stronger coupled effect between the moving particles and gas phase with a smaller Stokes number at mesh 2 (see Table 2) and a weaker contribution of moving particles on the source terms that are present into the differential equations of the gaseous phase ($\sum_p m_p((u_p)_{out} - (u_p)_{in})/(V_{cell}\Delta t)$, where $(u_p)_{in}$, $(u_p)_{out}$ are velocities of particles moving in and out of a cell with volume V_{cell}) , when the grid is more refined.

Another interesting result in terms of mixture formation ahead of the combustion process is that in mesh 1 the grid refinement leads to pockets of high vapour penetration travelling longer protected in the core of the spray while for mesh 2 the vapour is diffused more and thus high fuel vapour mainly exists up to $20mm$. This difference in the vapour distribution is expected to affect the combustion mode that will be observed in the simulations. In mesh 1 the combustion is expected to be dominated by non-premixed mode dynamics while in mesh 2 it will be premixed.

Conclusions

The present work is focused on the effect of the grid size refinement on spray evaporation and mixture formation in LES using Eulerian-Lagrangian approaches. The grid size apart from its profound role on resolving turbulent scales for the Eulerian phase, it also affects the way the parcels move and how often the momentum equation is updated. It is expected that for smaller grid sizes the parcel properties are updated in shorter time scales than in larger grids. As the grid is refined, the results for global liquid and vapour penetration demonstrate convergence toward the experimental data. However, this is not necessarily indicative of the overall accuracy of the simulations since, depending on the refinement areas, the droplet statistics are altered. More experimental data relevant to droplet sizes and velocities are required though for more solid conclusions. For both mesh cases examined in this study, as the grid size is refined the droplet trajectories are becoming longer along the direction of fuel mass injection and more fuel particles with higher particle velocities are present. In terms of the area of mesh refinement, the mesh refinement along direction of mass flow injection improves importantly the development of small scales of gas phase, which also alters the droplet size distribution and the overall droplet number although the overall mass exchanged does not change. Finally, since for multiphase flows the Kolmogorov scale cannot be considered as the only smallest flow scale and be used as scale separation criterion for the grid selection in a similar way done for single phase flows, the numerical Stokes number can play the role of an additional grid selection parameter. Further analysis is required towards this direction.

Acknowledgements

This work was supported by the UK's Engineering and Physical Science Research Council through the grant EP/P012744/1.

References

[1] Bravo, L. and Kweon, C.-B., "Numerical Simulations of Evaporating Sprays in High Pressure and Temperature Operating Conditions (Engine Combustion Network [ECN])", U.S. Army Research Laboratory, May 2014

[2] Mustafa, K. and Nsikane, D. and Ward, A. and Morgan, R. and Mason, D. and Heikal, M., "Statistical approach on visualizing multi-variable interactions in a hybrid breakup model under ECN spray condition", *SAE International Journal of Engines* 10 (5): 2461-2477 (2017)

[3] Bolla, M. and Chishty, M. A. and Hawkes, E. R. and Kook, S., "Modeling combustion under engine combustion network Spray A conditions with multiple injections using the transported probability density function method", *International Journal of Engine Research*, 18(1-2) 6-14, 2017

[4] Banerjee, S. and Rutland, C., "On LES Grid Criteria for Spray Induced Turbulence", *SAE International*, 2012

[5] Som, S. and Senecal, P.K. and Pomraning, E., "Comparison of RANS and LES Turbulence Models against Constant Volume Diesel Experiments", *ILASS Americas, 24th Annual Conference on Liquid Atomization and Spray Systems*, San Antonio, TX, May 2012

[6] Xue, Q. and Som, S. and Senecal, P.K. and Pomraning, E., "A Study of Grid Resolution and SGS Models for LES under Non-reacting Spray Conditions", *ILASS Americas, 25th Annual Conference on Liquid Atomization and Spray Systems*, Pittsburgh, PA, May 2013

[7] Wehrfritz, A. and Vuorinen, V. and Kaario, O. and Larmi, M., "A High Resolution Study of Non-Reacting Fuel Sprays using Large-Eddy Simulations", *ICLASS 2012, 12 th Triennial International Conference on Liquid Atomization and Spray Systems*, Heidelberg, Germany, September 2-6, 2012

[8] Vogiatzaki, K. and Crua, C. and Morgan, R. and Heikal, M., "A study of the controlling parameters of fuel air mixture formation for ECN Spray A", *Proceedings ILASS 2017* (2017)

[9] Greifzu, F. and Kratzsch, C. and Forgber, T. and Lindner, F. and Schwarze, R., "Assessment of particle-tracking models for dispersed particle-laden flows implemented in OpenFOAM and ANSYS FLUENT", *Engineering Applications of Computational Fluid Mechanics*, 10:1, 30-43, 2016

[10] Reitz, R. D., "Modeling Atomization Processes in High Pressure Vaporizing Sprays", *Atomization and Spray Technology* 3:309-337 (1987)

[11] Patterson, M. A. and Reitz, R. D., "Modeling the Effects of Fuel Spray Characteristics on Diesel Engine Combustion and Emissions", *SAE Paper* No. 980131 (1998).

[12] Spalding, D. B., "The Combustion of Liquid Fuels", *Proceedings of the 4 th Symposium (International) on Combustion*, The Combustion Institute, 847-864 (1953)

[13] Sandia Laboratories, *Engine Combustion Network*, `https://ecn.sandia.gov/`, (2017).

[14] Hirt, C. W. and Nichols, B. D., Volume of fluid (VOF) method for the dynamics of free boundaries, *Journal of Computational Physics* 39: 201-225 (1981)